J Nanopart Res (2013) 15:1432
DOI 10.1007/s11051-013-1432-9

RESEARCH PAPER

Comparison of TiO_2 and ZnO nanoparticles for photocatalytic degradation of methylene blue and the correlated inactivation of gram-positive and gram-negative bacteria

Robert J. Barnes · Rodrigo Molina · Jianbin Xu · Peter J. Dobson · Ian P. Thompson

Received: 25 July 2012 / Accepted: 11 January 2013 / Published online: 22 January 2013

Abstract Titanium dioxide (TiO_2) and zinc oxide (ZnO) nanoparticles are important photocatalysts and as such have been extensively studied for the removal of organic compounds from contaminated air and water and for microbial disinfection. Despite much research on the effect of TiO_2 and ZnO nanoparticles on different bacterial species, uncertainties remain about which bacteria are more sensitive to these compounds. Very few studies have directly compared the toxicity of ZnO to TiO_2 under both light and dark conditions. In addition, authors investigating the photocatalytic inactivation of TiO_2 and ZnO nanoparticles on bacteria have failed to investigate the reactive oxygen species (ROS) generation of the nanoparticles, making it difficult to correlate killing action with the generation of ROS. In this study, three types of metal nanoparticle ($ZnO < 50$ nm, $ZnO < 100$ nm and TiO_2) have been characterised and ROS production assessed through the degradation of methylene blue (MB). The photocatalytic killing potential of three nanoparticle concentrations (0.01, 0.1 and 1 g/L) was then assessed on four representative bacteria: two gram-positive (*S. aureus* and *B. subtilis*) and two gram-negative (*E. coli* and *P. aeruginosa*). Results showed that out of the three nanoparticles tested, the TiO_2 nanoparticles generated more ROS than the ZnO nanoparticles, corresponding to a greater photocatalytic inactivation of three of the four species of bacteria examined. The MB decomposition results correlated well with the bacterial inactivation results with higher TiO_2 nanoparticle concentrations leading to greater ROS production and increased loss of cell viability. Although producing less ROS than the TiO_2 nanoparticles under ultraviolet light, the ZnO nanoparticles were toxic to two of the bacterial species even under dark conditions. In this study, no correlation between cell wall type and bacterial inactivation was observed for any of the nanoparticles tested although both gram-positive bacteria were sensitive to ROS production. *P. aeruginosa* cells were resistant to all types of treatment and highlight a potential limitation to the application of these nanoparticles for water treatment.

Keywords Nanoparticles · Metal oxides · Reactive oxygen species · Toxicity · Bacteria · Photocatalysis

R. J. Barnes · R. Molina · J. Xu · I. P. Thompson (✉)
Department of Engineering Science, Oxford University, Parks Road, Oxford OX1 3PJ, UK
e-mail: Ian.Thompson@eng.ox.ac.uk

P. J. Dobson
Begbroke Directorate, Oxford University Begbroke Science Park, Sandy Lane OX5 1PF, UK

Introduction

Nanoscale titanium dioxide (TiO_2) and zinc oxide (ZnO) particles have global importance as opacifiers,

absorbers of ultraviolet (UV) light and broad scale use as pigments in paints, plastics, paper coatings and sunscreen lotions. Both of these materials are important photocatalysts and as such have been extensively studied for the removal of organic compounds from contaminated air and water and for microbial disinfection (Hoffmann et al. 1995; Byrne et al. 1998; Gaswami et al. 1997; Wei et al. 1994; Muggli and Ding 2001; Fu et al. 2005; Maness et al. 1999; Adams et al. 2006; Hariharan 2006).

When a TiO_2 or ZnO photocatalyst is irradiated with light of energy greater than or equal to its band gap, electron–hole pairs are generated that induce redox reactions at its surface. Through the reduction of oxygen by electrons and oxidation of water or hydroxide ions by photogenerated holes, this photocatalytic reaction gives rise to reactive oxygen species (ROS), including hydroxyl radicals, hydrogen peroxide and superoxide ions (Linsebigler et al. 1995; Maness et al. 1999). Since ZnO has almost the same band gap energy as TiO_2, their photocatalytic capacity is anticipated to be similar. However, in the case of ZnO, photocorrosion frequently occurs with the illumination of UV light, leading to a decrease of photocatalytic activity in aqueous solutions (Hariharan 2006).

The ROS generated by TiO_2 and ZnO nanoparticles may oxidise organic contaminants, and can cause fatal damage to microorganisms by disrupting or damaging various cell functions or structures (Maness et al. 1999; Jacoby et al. 1998; Legrini et al. 1993; Linsebigler et al. 1995). For a contaminant or cell in contact with the TiO_2 or ZnO photocatalyst surface, there may also be direct electron or hole transfer (Blake et al. 1999). Upon their production on the nanoparticle surface, both hydroxyl radicals and superoxide ions interact immediately with the outer surface of the organism. This can result in cell wall damage and subsequent peroxidation of the polyunsaturated phospholipid component of the lipid membrane (Maness et al. 1999). However, if the nanoparticles are small enough to penetrate the cell, these processes may occur internally. Compared to hydroxyl radicals and superoxide ions, hydrogen peroxide is less detrimental. However, hydrogen peroxide can enter the cell and be activated by ferrous ion via the Fenton reaction, leading to the production of the more damaging hydroxyl radicals (Blake et al. 1999). Since the initial actions of these ROS target the outer surface of a cell, the rigidity and chemical arrangements of their surface structure will determine how effectively the photocatalytic disinfection process functions (Blake et al. 1999).

Despite much research on the effect of TiO_2 and ZnO nanoparticles on different bacterial species, uncertainties remain about which bacteria are more sensitive to these compounds. Some authors have reported an equal inactivation of both gram-positive and gram-negative bacteria in the presence of irradiated TiO_2 nanoparticles (Tsuang et al. 2008). However, some authors have reported that gram-positive bacteria are less sensitive due to their ability to form spores (Wei et al. 1994; Rincon and Pulgarin 2005), whilst others have found contradictory results (Adams et al. 2006; Fu et al. 2005). There is also uncertainty about the toxicity of TiO_2 nanoparticles to bacteria when not irradiated by UV light. Some authors have observed that cell death occurs in the dark (Adams et al. 2006), whereas other authors have found the nanoparticles to be harmless under this condition (Jones et al. 2008; Tsuang et al. 2008; Jiang et al. 2009). However, all authors agree that bacterial inactivation by TiO_2 nanoparticles is enhanced under UV illumination. ZnO has been shown to exhibit strong antibacterial activities on a broad range of bacteria (Liu et al. 2009; Sawai 2003; Adams et al. 2006; Jones et al. 2008; Huang et al. 2008; Tayel et al. 2011). Although the photocatalytic generation of ROS is considered to be one of the primary mechanisms of ZnO nanoparticle toxicity, a number of authors have shown these particles are toxic to bacterial cells under dark conditions (Tayel et al. 2011; Jiang et al. 2009; Adams et al. 2006). This suggests that penetration of the cell envelope and disorganisation of bacterial membrane is also likely to be a major contributing factor (Padmavathy and Vijayaraghavan 2008; Brayner et al. 2006; Liu et al. 2009; Huang et al. 2008). In addition, the toxic role of Zn^{2+} ions released from dissolution of ZnO is not clear. As with TiO_2, uncertainties remain on the sensitivity of different bacteria to ZnO nanoparticles. Some authors have shown an equal inactivation of gram-positive and gram-negative bacteria when employing ZnO nanoparticles (Jiang et al. 2009). However, it should be noted that in the study by Jiang et al., gram-positive bacteria were more sensitive than the gram-negative bacteria to bulk ZnO. The greater sensitivity of gram-positive bacteria to ZnO nanoparticles in comparison

to gram-negative bacteria has been commonly observed (Tayel et al. 2011; Sawai et al. 1995; Adams et al. 2006; Premanathan et al. 2011). Loss of viability has also correlated strongly with ZnO nanoparticle concentration (Adams et al. 2006; Liu et al. 2009). Very few studies have directly compared the toxicity of ZnO to TiO_2 under both light and dark conditions. Under only dark conditions, Jiang et al. 2009 reported that ZnO nanoparticles were more toxic than TiO_2 nanoparticles for all three bacteria studied. A study by Adams et al. 2006, showed a more complex scenario with toxicity being dependent on bacterial species. Under dark conditions, ZnO nanoparticles were more toxic to *B. subtilis* than TiO_2 nanoparticles, but the reverse was seen for *E. coli*. Under light conditions, the ZnO remained more toxic than the TiO_2 to the *B. subtilis*, but the TiO_2 and ZnO were of similar toxicity to *E.coli*. The concentration of nanoparticles was also seen to affect cell toxicity, where under light conditions a higher TiO_2 concentration of nanoparticles was required in comparison to ZnO for equal inactivation (Adams et al. 2006).

Contradictory results are likely a reflection of differing methodologies (e.g. exposure time and method, bacterial species, nanoparticle manufacturer, nanoparticle size, concentration of bacteria and nanoparticles, UV intensity and inhibition of growth vs. toxicity).

Previously, authors investigating the photocatalytic inactivation of TiO_2 and ZnO nanoparticles on bacteria have failed to investigate the ROS generation of the particles. This makes it difficult to correlate killing action with generation of ROS. ROS generation of photocatalytic nanoparticles is commonly assessed through the photodecomposition of methylene blue (MB) (Lakshmi et al. 1995; Xu et al. 1999; Kwon et al. 2004), although other methods have also been used (Qamar and Muneer 2009). Positive correlation between the degradation of methylene blue and inactivation of bacterial species is expected as the formation of hydroxyl radicals under UV illumination have been proposed as the dominant ROS responsible for both the photocatalytic degradation of organic compounds (Turchi and Ollis 1990) and the inactivation of bacterial cells (Cho et al. 2004).

The aim of this study was to characterise three types of metal oxide nanoparticle [ZnO <50 nm (ZnO_{50}), ZnO <100 nm (ZnO_{100}) and TiO_2] and to compare ROS production under UV activation (365 nm) through the degradation of MB. The photocatalytic inactivation potential of these nanoparticles was then assessed on four representative bacteria: two gram-positive (*S. aureus* and *B. subtilis*) and two gram-negative (*E. coli* and *P. aeruginosa*).

Materials and methods

Reagents

The TiO_2 nanoparticles (P25 formulation) were manufactured by Degussa Chemical Company (Germany). The ZnO nanoparticles (ZnO_{50} and ZnO_{100}) and phosphate-buffered saline (PBS) (0.01 M, pH 7.4) were purchased from Sigma-Aldrich (Gillingham, UK). The MB powder was purchased from Fisher Scientific (Loughborough, UK).

Analytical techniques

X-ray diffraction (XRD) analysis was carried out using a fully automated Siemens D5000 powder diffractometer employing copper k-alpha radiation (wavelength = 0.15406 nm) and a secondary monochromator. The sample was continuously spun during data collection and was scanned using a step size of 0.05 degrees two theta between the range of 20–80° two theta and a count time of 12 s per step. A generator voltage of 40 kV and tube current of 40 mA was used for the data acquisition. Siemens Diffrac plus (EVA version 8.0) software was used to display diffractograms and to identify the constituents.

High resolution transmission electron microscope (HRTEM) images were obtained using a JEOL 2010 HRTEM operating at 200 kV.

Zeta potential of suspended nanoparticles was determined using a Zetasizer Nano ZS (Malvern Instruments Ltd., Malvern, UK). Measurements were performed in triplicate at 25 °C with an equilibration time of 1 min in disposable capillary cells (Malvern Instruments Ltd., Malvern, UK) in an automatic mode.

Particle size distribution was measured using a CPS Disc Centrifuge (Model DC24000, CPS Instruments, Inc.), operated at a speed of 18500 rpm. A sucrose gradient was injected into the spinning disc using 24 % (w/v) and 8 % (w/v) sucrose solutions and subsequently sealed by injecting 0.5 ml of dodecane. A polyvinyl chloride (PVC) standard of 0.377 μm in deionised water solution was used for calibration.

BET specific surface area was measured by the nitrogen adsorption method (5 point isotherm) using a Micrometrics Gemini VI Surface Area and Pore Size Analyzer.

MB concentration was calculated according to the absorption at 630 nm measured by a microplate reader (Synergy HT, BioTek, USA). The extinction coefficient of MB at 630 nm was determined by a serial dilution of standards with known concentrations.

Preparation of bacterial cells

Liquid cultures of *Escherichia coli* (NCTC 10418) and *Bacillus subtilis* (NCTC 10400) were grown aerobically in nutrient broth (Oxoid) at 37 °C on a rotatory platform at 120 rpm for 24 h. Liquid cultures of *Pseudomonas aeruginosa* (NCTC 12934) and *Staphylococcus aureus* (NCTC 12981) were grown aerobically in tryptone soya broth (Oxoid) under the same conditions. Bacteria were harvested by centrifugation at $3{,}063\times g$ for 30 min, washed twice in sterile phosphate-buffered saline (PBS) (pH 7.4) and resuspended in PBS. The bacteria concentrations for experimental work were determined by a viable count procedure on nutrient agar (*E. coli* and *B. subtilis*) or tryptone soya agar (*P. aeruginosa* and *S. aureus*) (Oxoid) plates after serial dilutions of the cultures in PBS. Concentrations were chosen that would yield approximately 100 bacterial colonies per plate. Stock solutions of these bacterial concentrations (10^3 colony forming units (CFU)/ml) were then made up and used for all experimental work. This concentration of bacterial cells has previously been reported to allow substantial inactivation when employing UV-irradiated TiO_2 (Maness et al. 1999).

Experimental design

The photocatalytic experiments were carried out as previously reported (Johnson et al. 2011). In brief, stock aqueous TiO_2 or ZnO nanoparticle suspensions (20, 2 and 0.2 g/L in sterile deionised water) were prepared and immediately sonicated for 1 h in the dark before the photocatalytic reaction. 2 ml of each stock suspension was then added to 100-ml sterile glass beakers containing 38 ml of the relevant bacterial suspension to give nanoparticle concentrations of 1, 0.1 and 0.01 g/L. A UV control was also set up using 2 ml sterile deionised water in place of the aqueous TiO_2 nanoparticle suspension. All experimental conditions were run in triplicate. The beakers were placed on a magnetic stir plate with continuous stirring (to ensure maximal mixing and to prevent settling of the nanoparticles) and illuminated using a UV lamp (LF-206.LS, UVIlite ultraviolet lamp, Uvitec, UK) from above for 1 h, a duration similar to previous studies (Tsuang et al. 2008; Wei et al. 1994; Maness et al. 1999). The peak wavelength of the lamp was 365 nm. UV light intensity was measured using a low power photodetector (918 series, Newport, USA) and picoammeter (model 6485, Keithley, USA). The light intensity reaching the surface of the suspensions was approximately 4.2 W/m^2. The temperature of the suspensions was taken at the first and last time point to test that this parameter remained constant. A control (no nanoparticles or UV) and dark control (1 g/L nanoparticles without UV) were also set up. At each time point (0, 20, 40 and 60 min), 100 µl of suspension was removed from the beaker and spread on nutrient agar (*E. coli* and *B. subtilis*) or tryptone soya (*P. aeruginosa* and *S. aureus*) (Oxoid). Three replicates were produced for each plate. Plates were incubated at 37 °C (±2 °C) for 24 h before counting. The inactivation percentage was calculated by comparing the average CFU percentage change of the treated solutions with that of the control (no nanoparticles or UV).

Photocatalytic decomposition of methylene blue (MB)

The photocatalytic activity of different concentrations of TiO_2 and ZnO nanoparticles was examined by their photocatalytic decomposition of MB. The experimental design was set up as above, replacing the bacterial suspension with MB solution (20 mg/L). At each time point, 600 µl of suspension was removed and centrifuged (relative centrifugal force of $16{,}110\times g$ for 10 min) to remove the nanoparticles from solution before the absorbance was read. The concentration of MB after photocatalytic decomposition was determined by the absorption at 630 nm. All experimental conditions were carried out in triplicate. The percentage degradation was calculated by comparing the average absorbance (600 nm) percentage change of the treated solutions with that of the control (no nanoparticles or UV).

Results

Nanoparticle characterisation

Images acquired by TEM indicated that the TiO_2 nanoparticles were 10–100 nm in diameter with spherical or pseudo-spherical form (Fig. 1a). Particle size distribution analysed by weight is presented in Table 1. Particle agglomeration in solution caused a significant amount (>80 %) of nanoparticles to have a combined diameter >100 nm with a mean average size of 368.2 nm (Table 1). The mean particle size of metal oxide nanoparticles increasing once in suspension has been previously reported (Adams et al. 2006). Owing to their small size, the TiO_2 nanoparticles had a BET specific surface area of 49.73 m^2/g. X-ray diffraction (XRD) analysis of the TiO_2 nanoparticles showed that the material was a mixture of phases with a composition of 74.4 % anatase and 25.6 % rutile. The average zeta potential of the TiO_2 nanoparticles in deionised water was −29.0, showing that these particles are moderately unstable in aqueous suspension with flocculation observed to occur relatively quickly.

In comparison, TEM showed that the ZnO_{50} nanoparticles were predominantly smaller than 50 nm in diameter with spherical or pseudo-spherical form (Fig. 1b). However, some larger particles (or agglomerates of ZnO nanoparticles) were observed. Particle agglomeration in solution caused a significant amount (>40 %) of nanoparticles to have a diameter > 100 nm with a mean average size of 133.7 nm (Table 1). Despite being smaller than the TiO_2 nanoparticles, the ZnO_{50} nanoparticles had a smaller BET specific surface area of 22.58 m^2/g. XRD analysis showed a composition of 66.74 % Zincite, ZnO and a mixture of phases, including Gahnite $ZnAl_2O_4/ZnO{\cdot}Al_2O_3$ and Willemite Zn_2SiO_4. The average zeta potential of the ZnO_{50} nanoparticles in deionised water was -10.0 mV indicating that these particles are highly unstable in aqueous suspension at neutral pH, with rapid flocculation occurring. TEM images showed that the ZnO_{100} nanoparticles exhibited spherical or pseudo-spherical form and were predominantly smaller than 100 nm in diameter (Fig. 1c). Particle agglomeration in solution caused a significant amount (>90 %) of nanoparticles to have a diameter >100 nm with a mean average size of 260.2 nm (Table 1). The ZnO_{100} nanoparticles had a BET specific surface area of 12.09 m^2/g. XRD analysis of the ZnO_{100} nanoparticles showed a composition of 67.67 % Zincite, ZnO and a mixture of phases, including Gahnite $ZnAl_2O_4/ZnO{\cdot}Al_2O_3$ and Willemite Zn_2SiO_4. The average zeta potential of the ZnO_{100} nanoparticles was −22.0 mV. This result suggested that the ZnO_{100} nanoparticles are more stable in solution than the ZnO_{50} nanoparticles. The colloidal stability of the ZnO nanoparticles at neutral pH is relatively weak.

Degradation of methylene blue (MB)

The results indicate that the higher the concentration of nanoparticle, the greater the decomposition of MB (Table 2). The 1 g/L TiO_2 nanoparticle suspension with UV resulted in a 76 % reduction in absorbance after 1 h, indicating that these particles generate a large amount of ROS during UV activation. However,

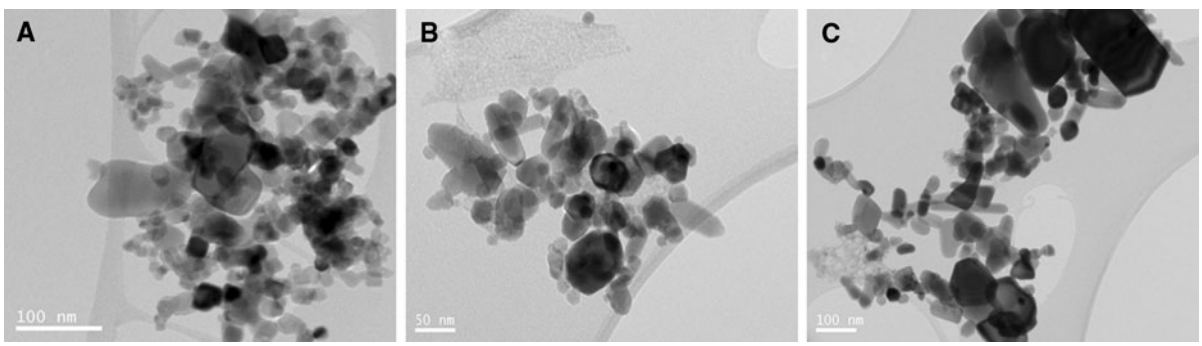

Fig. 1 TEM image of **a** TiO_2 nanoparticles—100 nm scale, **b** ZnO_{50} nanoparticles—50 nm scale, **c** ZnO_{100} nanoparticles—100 nm scale

Table 1 Size distribution of particles by weight (% fraction), determined by CPS disc centrifuge

Nanoparticle type	0–93 nm	93–142 nm	142–219 nm	219–336 nm	336–516 nm	516–793 nm	793–1874 nm	Mean average particle size (nm)
TiO_2	13.94	18.81	15.88	12.39	13.57	12.24	11.94	401.8
	14.37	19.78	16.50	12.87	14.30	12.28	9.65	352.2
	14.40	20.04	16.39	12.78	14.63	12.29	9.11	350.6
Average ($n = 3$)	14.24	19.54	16.26	12.68	14.17	12.27	10.23	368.2
ZnO_{50}	51.46	30.12	12.43	3.12	1.75	0.86	0.23	126.4
	46.67	30.04	15.8	4.23	2.1	0.90	0.24	135.4
	43.16	31.85	17.2	4.58	2.14	0.86	0.19	139.3
Average ($n = 3$)	47.10	30.67	15.14	3.98	2.00	0.87	0.22	133.7
ZnO_{100}	5.21	15.23	33.91	32.24	10.9	1.98	0.53	256.5
	4.42	13.79	32.76	35.82	10.86	1.61	0.66	263.4
	4.40	12.58	31.87	38.6	10.87	1.25	0.42	260.7
Average ($n = 3$)	4.68	13.87	32.85	35.55	10.88	1.61	0.54	260.2

it should be noted that although only one tenth the concentration, the 0.1 g/L UV illuminated TiO_2 nanoparticle suspension degraded a very similar concentration of MB over the experimental period (74 %). The greater amount of solids in the 1 g/L TiO_2 nanoparticle suspension may therefore have increased UV shading to the point of inhibiting photocatalytic activity, as has been previously reported (Maness et al. 1999). The 0.01 g/L TiO_2 suspension resulted in only a small percentage reduction in MB absorbance (22 %). The largest MB degradation occurred between 0 and 20 min (69, 55 and 16 % for the 1, 0.1 and 0.01 g/L respectively). A comparison of the ZnO nanoparticles showed that the ZnO_{100} suspension degraded a higher percentage of MB than the ZnO_{50} suspension for all concentrations tested (Table 2). However, both types of ZnO nanoparticle produced a lower amount of ROS than that of equal concentrations of the TiO_2 nanoparticles. There were no significant changes in the control (no nanoparticles and no UV), dark control and UV control MB solution absorbance, indicating that nanoparticles not activated with UV did not generate ROS. In addition, UV alone did not degrade MB.

Table 2 Summary of results for degradation of methylene blue employing different concentrations of TiO_2 and ZnO nanoparticles under UV light (365 nm)

Nanoparticle concentration (g/L)	% methylene blue degraded after 1 h exposure		
	TiO_2	ZnO_{50}	ZnO_{100}
1	76 (4)	18 (3)	29 (6)
0.1	74 (2)	7 (2)	16 (2)
0.01	22 (6)	1 (1)	2 (1)
UV control	0	0	0
Dark control	0	0	0

UV control—UV exposure without nanoparticles. Dark control—1 g/L nanoparticles without UV exposure

Values in parentheses are standard deviation, $n = 9$

Impact of TiO_2 nanoparticles (with and without UV) on the survival of 4 representative bacterial strains

Results for *E. coli* showed that UV alone and TiO_2 nanoparticles without UV activation had no negative impact on cell viability (Table 3). However, 1, 0.1 and 0.01 g/L TiO_2 nanoparticle concentrations with UV illumination resulted in 100, 100 and 27 % inactivation, respectively. The largest inactivation occurred between 0 and 20 min (71, 71 and 21 % respectively), corresponding to the MB degradation experiment. Although only one tenth the concentration, the 0.1 g/L UV illuminated TiO_2 nanoparticle suspension inactivated a similar percentage of bacterial cells as the 1 g/L suspension over the experimental period. The greater amount of solids in the 1 g/L TiO_2 nanoparticle suspension may therefore have increased UV shading to the point of inhibiting photocatalytic activity, as has been previously reported (Maness et al. 1999). Owing to lower cost of using a lesser concentration of nanoparticles, 0.1 g/L is selected as the optimum concentration for inactivation of *E. coli* cells in a water purification system.

Results for *S. aureus* showed that no loss of viability occurred with TiO_2 nanoparticles without UV activation (Table 3). However, 1, 0.1 and 0.01 g/L TiO_2 nanoparticle concentrations with UV illumination resulted in a 90, 80 and 51 % inactivation, respectively, of the *S. aureus* cells. Although only one tenth the concentration, the 0.1 g/L UV-illuminated TiO_2 nanoparticle suspension inactivated a similar percentage of bacterial cells as the 1 g/L suspension, which can once again be attributed to UV shading by the greater nanoparticle concentration. Interestingly, UV (365 nm) alone killed 31 % of the bacterial cells, indicating that *S. aureus* cells were more sensitive to UV than the *E. coli* cells.

The results indicated that *P.aeruginosa* cells were highly resistant to inactivation by UV-activated TiO_2

Table 3 Summary of results for bacterial inactivation employing different concentrations of TiO_2 and ZnO nanoparticles under UV light (365 nm)

Bacterial species	Nanoparticle concentration (g/L)	% bacterial cells inactivated after 1 h exposure		
		TiO_2	ZnO_{50}	ZnO_{100}
E. coli	1	100	30 (9)	35 (2)
	0.1	100	21 (9)	24 (6)
	0.01	27 (6)	18 (5)	20 (10)
	UV control	0	0	0
	Dark control	0	21 (8)	24 (4)
S. aureus	1	90 (2)	34 (5)	47 (12)
	0.1	80 (6)	23 (6)	32 (6)
	0.01	51 (2)	22 (10)	28 (10)
	UV control	31 (3)	27 (7)	26 (4)
	Dark control	0	0	0
P. aeruginosa	1	0	0	0
	0.1	0	0	0
	0.01	0	0	0
	UV control	0	0	0
	Dark control	0	0	0
B. subtilis	1	100	100	100
	0.1	100	87 (4)	90 (2)
	0.01	96 (1)	82 (2)	84 (4)
	UV control	67 (3)	70 (5)	68 (3)
	Dark control	0	100	100

UV control—UV exposure without nanoparticles. Dark control—1 g/L nanoparticles without UV exposure

Values in parentheses are standard deviation, $n = 9$

nanoparticles. No significant loss of viability was observed over the duration of the experiment with any nanoparticle concentration (Table 3).

For *B. subtilis*, no bacterial inactivation occurred with TiO_2 nanoparticles without UV activation (Table 3). However, 1, 0.1 and 0.01 g/L TiO_2 nanoparticle concentrations with UV illumination resulted in 100, 100 and 96 % inactivation, respectively. UV alone inactivated 67 % of the bacterial cells, indicating that out of the four bacterial species tested, *B. subtilis* cells were the most sensitive to UV light intensity.

In all experiments, the temperature of the suspensions remained constant throughout the 60-min illumination period, showing that an increase in temperature was not responsible for any loss of bacterial viability.

Impact of ZnO_{50} nanoparticles (with and without UV) on the survival of 4 representative bacterial strains

Results for *E. coli* showed that no cell inactivation occurred with UV light alone. However, 1, 0.1 and 0.01 g/L ZnO_{50} nanoparticle concentrations with UV illumination resulted in a 30, 21 and 18 % inactivation, respectively. Interestingly, 21 % of the *E. coli* cells were inactivated by the ZnO_{50} dark control, showing that these particles were toxic to bacterial cells even without UV activation. The bacterial toxicity of ZnO nanoparticles under dark conditions has been previously reported (Tayel et al. 2011; Jiang et al. 2009; Adams et al. 2006). In comparison to the TiO_2 nanoparticle results, under UV activation, the ZnO_{50} nanoparticles inactivated significantly less *E. coli* cells. This can be attributed to them producing less ROS, as observed in the MB degradation experiments.

S. aureus cells were relatively resistant to UV activated ZnO_{50} nanoparticles. UV alone inactivated 27 % of the bacterial cells with only a small increase in cell kill observed in the presence of 1 g/L ZnO_{50} nanoparticles (Table 3). This is an unusual result, as a high sensitivity of *S. aureus* to ZnO nanoparticles has been previously reported (Tayel et al. 2011; Premanathan et al. 2011; Jones et al. 2008). However, in previous studies, the ZnO has either been used for growth inhibition rather than for direct inactivation or toxicity has been assessed over exposure times greater than 1 h.

The results indicated that *P. aeruginosa* cells were highly resistant to inactivation by both UV- and non-UV-activated ZnO_{50} nanoparticles. No significant inactivation was observed over the duration of the experiment with any nanoparticle concentration (Table 3).

Results for *B. subtilis* showed that no loss of viability occurred in the control (Table 3). This bacterial species once again showed high sensitivity to the UV light with a 70 % inactivation being observed in the UV control. Interestingly, 100 % *B. subtilis* cells were inactivated immediately after 1 g/L nanoparticles were added (1 g/L and dark control), indicating that *B. subtilis* cells were highly sensitive to ZnO_{50} nanoparticles. The 0.1 and 0.01 g/L ZnO nanoparticle concentrations with UV illumination resulted in an 87 % and 82 inactivation, respectively, of the *B. subtilis* cells, but this is attributed mostly to the effect of the UV and toxic effect of the ZnO nanoparticles, rather than through generation of ROS.

Impact of ZnO_{100} nanoparticles (with and without UV) on the survival of 4 representative bacterial strains

Results for *E. coli* showed that UV light alone had no negative effect on bacterial viability (Table 3). However, 1, 0.1 and 0.01 g/L ZnO_{100} nanoparticle concentrations with UV illumination resulted in a 35, 24 and 20 % inactivation, respectively. Similar to the ZnO_{50} nanoparticles, 24 % of the *E. coli* cells were inactivated by the ZnO_{100} dark control (1 g/L), showing that these particles were toxic to bacterial cells even without UV activation. In comparison to the TiO_2 nanoparticle results, under UV activation, the ZnO_{100} nanoparticles inactivated significantly less *E. coli* cells. However, the ZnO_{100} and the ZnO_{50} nanoparticles inactivated a similar percentage of bacterial cells (35 and 30 %, respectively).

No loss of *S. aureus* cell viability occurred without UV light. However, 1, 0.1 and 0.01 g/L ZnO_{100} nanoparticle concentrations with UV illumination resulted in a 47, 32 and 28 % inactivation, respectively (Table 3). 26 % of *S. aureus* cells were killed by UV alone. In comparison to the ZnO_{50} nanoparticle results, ZnO_{100} nanoparticles inactivated a higher percentage of *S. aureus* cells under UV activation, likely due to the greater production of ROS.

P. aeruginosa cells were highly resistant to inactivation by UV activated ZnO_{100} nanoparticles. No

significant loss of viability was observed over the duration of the experiment with any nanoparticle concentration.

Results for *B. subtilis* showed that no bacterial inactivation occurred in the control (Table 3). Similar to the previous two experiments, this bacterial species showed high sensitivity to the UV light with a 68 % inactivation being observed in the UV control. 100 % of the *B. subtilis* cells were inactivated immediately after addition of 1 g/L nanoparticles (1 g/L and dark control), indicating *B. subtilis* cells were also highly sensitive to ZnO_{100} nanoparticles. The 0.1 and 0.01 g/L ZnO nanoparticle concentrations with UV illumination resulted in a 90 and 84 % inactivation, respectively, of the *B. subtilis* cells, but this is attributed mostly to the affect of the UV and toxic effect of the ZnO nanoparticles, rather than through generation of ROS.

Discussion

Despite having a larger mean particle size in solution than both ZnO nanoparticles, the TiO_2 nanoparticles generated more ROS, corresponding to a greater photocatalytic killing of three of the four species of bacteria examined. Greater ROS production by TiO_2 nanoparticles in comparison to ZnO nanoparticles has been previously reported (Qamar and Muneer 2009). This is likely because of the vulnerability of ZnO nanoparticles to photocorrosion leading to a decrease of ZnO photocatalytic activity in aqueous solutions (Hariharan 2006). The MB decomposition results correlated well with the bacterial inactivation results with the 0.1 and 1 g/L TiO_2 nanoparticle suspensions producing similar amounts of ROS and killing a like percentage of bacterial cells. Although 0.01 g/L TiO_2 nanoparticles were able to only produce a small amount of ROS ($\sim$22 % reduction in MB absorbance), this concentration of nanoparticle also led to bacterial photocatalytic kill up to 27 % in the case of the *E. coli* cells. Positive correlation between the degradation of methylene blue and inactivation of bacterial species is likely to have been observed because of the dominant role of hydroxyl radicals in both the photocatalytic degradation of organic compounds (Turchi and Ollis 1990) and the inactivation of bacterial cells (Cho et al. 2004). The TiO_2 nanoparticles were not toxic without UV activation, as previously reported (Jones et al. 2008; Tsuang et al. 2008; Jiang et al. 2009). This shows that the production of ROS by the irradiated TiO_2 nanoparticles was the main action of inactivation. The ZnO_{100} nanoparticles were shown to be less photocatalytic than the TiO_2 nanoparticles, but more photocatalytic than the ZnO_{50}. This is interesting, as a smaller particle size would be expected to be more reactive. However, the ZnO_{50} nanoparticles were of lower purity than those of the ZnO_{100} and contained 6 % Al as a dopant, both of which could have affected the photocatalytic potential. The difference in ROS generation between the ZnO nanoparticles corresponds with a higher inactivation percentage being achieved for *S. aureus* with the ZnO_{100} nanoparticles. However, the inactivation percentages for both types of ZnO nanoparticle were shown to be similar for both *B. subtilis* and *E. coli*. This is likely because the particles were toxic to these bacterial strains even without UV activation, meaning that the impact of ROS generation on cell inactivation was less significant. Cell inactivation by ZnO nanoparticles under dark conditions has previously been shown to increase as the nanoparticle size decreases (Padmavathy and Vijayaraghavan 2008). However, in this study the inactivation percentage of *E. coli* cells was the same for both ZnO nanoparticles. This may again be attributed to the lower purity of the ZnO_{50} nanoparticles in comparison to that of the ZnO_{100}. The *B. subtilis* was more sensitive to the presence of ZnO nanoparticles under dark conditions than the *E.coli*, as has been previously reported (Adams et al. 2006). Results under UV irradiation are difficult to compare due to the *B. subtilis* being sensitive to UV light. Interestingly, despite both gram-positive bacteria being sensitive to ROS production, in this study, no correlation between cell wall type and ROS-influenced bacterial inactivation was observed. An example of this is the large difference in inactivation rate between the gram-negative *E. coli* and *P. aeruginosa*. Despite both being gram-negative, the *E. coli* was effectively inactivated by the TiO_2 nanoparticles during UV excitation, whereas the *P. aeruginosa* cells were highly resistant. This is an interesting result and shows that bacterial resistance to ROS generation is due to other factors. Although not assessed in this research, a potential factor could be the production of protective EPS. A recent study has shown that capsular EPS produced by *P. aeruginosa* provides a protective role for bacterial cells against regulatory residual

disinfectants by reducing membrane permeabilization (Xue et al. 2013). Thus, this EPS could act to protect this species of bacteria against ROS damage or membrane damage by ZnO nanoparticles. The resistance of this treatment by *P. aeruginosa* highlights a potential limitation to the application of these nanoparticles for water treatment. However, a higher UV intensity or longer exposure time is likely to generate more ROS which may lead to more significant kill of resistant bacteria. No correlation between cell wall type and bacterial inactivation was observed in the presence of ZnO nanoparticles, where both gram-negative *E. coli* and gram-positive *B. subtilis* were killed by the ZnO nanoparticles without UV activation and gram-positive *S. aureus* and gram-negative *P. aeruginosa* were not affected. Also interesting is that both gram-positive bacterial species were sensitive to UV (365 nm) light under experimental conditions. Despite this sensitivity, the *S. aureus* still had a lower inactivation rate in the presence of irradiated TiO_2 nanoparticles in comparison to *E. coli*.

Conclusions

TiO_2 and ZnO nanoparticles have been extensively characterised and a range of concentrations tested for degradation of MB (ROS generation) and correlated photocatalytic kill of four representative bacterial species (two gram-positive and two gram-negative).

TEM analysis revealed that the particles were of similar size to that advertised. However, the mean particle size of the tested nanoparticles increased once in suspension, attributed to their low zeta potential and consequential instability in solution at neutral pH.

Results showed that out of the three nanoparticles tested, the TiO_2 nanoparticles generated more ROS than the ZnO nanoparticles, corresponding to a greater photocatalytic killing of three of the four species of bacteria examined. The MB decomposition results correlated well with the bacterial inactivation results with higher TiO_2 nanoparticle concentrations leading to greater ROS production and superior inactivation. Although less photocatalytic, the ZnO nanoparticles were toxic to two of the bacterial species even under dark conditions. In this study, no correlation between cell wall type and bacterial inactivation was observed for any of the nanoparticles tested although both gram-positive bacteria were sensitive to ROS production. *P.aeruginosa* cells were resistant to all types of treatment and highlight a potential limitation to the application of these nanoparticles for water treatment.

Acknowledgments Research was supported by NERC. The authors also thank Xin Zhao and Frank Cullen of the Department of Materials, University of Oxford, for TEM and XRD analyses.

References

Adams LK, Lyon DY, Alvarez PJJ (2006) Comparative eco-toxicity of nanoscale TiO_2, SiO_2, and ZnO water suspensions. Water Res 40:3527–3532

Blake DM, Maness PC, Huang Z, Wolfrum EJ, Huang J (1999) Application of the photocatalytic chemistry of titanium dioxide to disinfection and the killing of cancer cells. Sep Purif Methods 28:1–50

Brayner R, Ferrari-Iliou R, Brivois N, Djediat S, Benedetti MF, Fiévet F (2006) Toxicological impact studies based on Escherichia coli bacteria in ultrafine ZnO nanoparticles colloidal medium. Nano Lett 6:866–870

Byrne JA, Eggins BR, Brown NMD, McKinnery B, Rouse M (1998) Immobilisation of TiO_2 powder for the treatment of polluted water. Appl Catal B 17:25–36

Cho M, Chung H, Choi W, Yoon J (2004) Linear correlation between inactivation of *E. coli* and OH radical concentration in TiO_2 photocatalytic disinfection. Water Res 38:1069–1077

Fu G, Vary PS, Lin C-T (2005) Anatase TiO_2 nanocomposites for antimicrobial coatings. J Phys Chem B 109:8889–8898

Gaswami DY, Trivedi DM, Block SS (1997) Photocatalytic disinfection of indoor air. J Sol Energy Eng 119:92–96

Hariharan C (2006) Photocatalytic degradation of organic contaminants in water ZnO by nanoparticles: revisited. Appl Catal A 304:55–61

Hoffmann MR, Martin ST, Choi W, Bahnemann DW (1995) Environmental applications of semiconductor photocatalysis. Chem Rev 95:69–96

Huang Z, Zheng X, Yan D, Yin G, Liao X, Kang Y, Yao Y, Huang D, Hao B (2008) Toxicological effect of ZnO nanoparticles based on bacteria. Langmuir 24:4140–4144

Jacoby WA, Maness PC, Wolfrum EJ, Blake DM, Fennel JA (1998) Mineralization of bacterial cell mass on a photocatalytic surface in air. Environ Sci Technol 32:2650–2653

Jiang W, Mashayekhi H, Xing B (2009) Bacterial toxicity comparison between nano- and micro-scaled oxide particles. Environ Pollut 157:1619–1625

Johnson AC, Bowes MJ, Crossley A, Jarvie HP, Jurkschat K, Jürgens MD, Lawlor AJ, Park B, Rowland P, Spurgeon D, Svendsen C, Thompson IP, Barnes RJ, Williams RJ, Xu N (2011) An assessment of the fate, behaviour and environmental risk associated with sunscreen TiO_2 nanoparticles in UK field scenarios. Sci Total Environ 409:2503–2510

Jones N, Ray B, Ranjit KT, Manna AC (2008) Antibacterial activity of ZnO nanoparticle suspensions on a broad spectrum of microorganisms. FEMS Microbiol Lett 279:71–76

Kwon CH, Shin H, Kim JH, Choi WS, Yoon KH (2004) Degradation of methylene blue via photocatalysis of titanium dioxide. Mater Chem Phys 86:78–82

Lakshmi S, Renganathan R, Fujita S (1995) Study on TiO_2-mediated photocatalytic degradation of methylene blue. A 88:163–167

Legrini O, Oliveros E, Braun AM (1993) Photochemical processes for water treatment. Chem Rev 93:671–698

Linsebigler AL, Lu G, Yates JT (1995) Photocatalysis on TiO_2 surfaces: principles, mechanisms, and selected results. Chem Rev 95:735–758

Liu Y, He L, Mustapha A, Li H, Hu ZQ, Lin M (2009) Antibacterial activities of zinc oxide nanoparticles against *Escherichia coli* O157:H7. J Appl Microbiol 107: 1193–1201

Maness PC, Smolinski S, Blake DM, Huang Z, Wolfrum EJ, Jacoby WA (1999) Bactericidal activity of photocatalytic TiO(2) reaction: toward an understanding of its killing mechanism. Appl Environ Microbiol 65:4094–4098

Muggli DS, Ding L (2001) Photocatalytic performance of sulfated TiO_2 and Degussa P-25 TiO_2 during oxidation of organics. Appl Catal B 32:181–194

Padmavathy N, Vijayaraghavan R (2008) Enhanced bioactivity of ZnO nanoparticles-an antimicrobial study. Sci Technol Adv Mater 9:035004

Premanathan M, Karthikeyan K, Jeyasubramanian K, Manivannan G (2011) Selective toxicity of ZnO nanoparticles toward Gram-positive bacteria and cancer cells by apoptosis through lipid peroxidation. Nanomedicine 7:184–192

Qamar M, Muneer M (2009) A comparative photocatalytic activity of titanium dioxide and zinc oxide by investigating the degradation of vanillin. Desalination 249:535–540

Rincon AG, Pulgarin C (2005) Use of coaxial photocatalytic reactor (CAPHORE) in the TiO_2 photo-assisted treatment of mixed *Escherichia coli* and *Bacillus subtilis* and the bacterial community present in wastewater. Catal Today 101:331–344

Sawai J (2003) Quantitative evaluation of antibacterial activities of metallic oxide powders (ZnO, MgO and CaO) by conductimetric assay. J Microbiol Methods 54:177–182

Sawai J, Igarashi H, Hashimoto A, Kokugan T, Shimizu M (1995) Effect of ceramic powders on spores of *Bacillus subtilis*. J. Chem. Eng. Japan 28:288–293

Tayel AA, El-Tras WF, Moussa S, El-Baz AF, Mahrous H, Salem MF, Brimer L (2011) Antibacterial action of zinc oxide nanoparticles against foodborne pathogens. J Food Saf 31:211–218

Tsuang YH, Sun JS, Huang YC, Lu CH, Chang WH, Wang CC (2008) Studies of photokilling of bacteria using titanium dioxide nanoparticles. Artif Organs 32:167–174

Turchi CS, Ollis DF (1990) Photocatalytic degradation of organic water contaminants: mechanisms involving hydroxyl radical attack. J Catal 122:178–192

Wei C, Lin WY, Zaina Z, Williams NE, Zhu K, Kruzic AP, Smith RL, Rajeshwar K (1994) Bactericidal activity of TiO_2 photocatalyst in aqueous media: toward a solar-assisted water disinfection system. Environ Sci Technol 28:934–938

Xu N, Shi Z, Fan Y, Dong J, Shi J, Hu MZ-C (1999) Effects of particle size of TiO_2 on photocatalytic degradation of methylene blue in aqueous suspensions. Ind Eng Chem Res 38:373–379

Xue Z, Hessler CM, Panmanee W, Hassett DJ, Seo Y (2013) *Pseudomonas aeruginosa* inactivation mechanism is affected by capsular extracellular polymeric substance reactivity with chlorine and monochloramine. FEMS Microbiol Ecol 83:101–111